



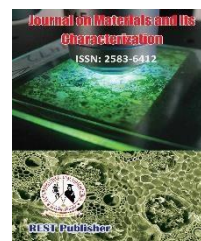
Journal on Materials and its Characterization

Vol: 2(2), June 2023

REST Publisher; ISSN: 2583-6412 (Online)

Website: <https://restpublisher.com/journals/jmc/>

DOI: <https://doi.org/10.46632/jmc/2/2/3>



Herbal extract stabilized fabrication of zirconia nanoparticles for compacting pathogenic bacteria and human cancer cells

S. Reni Florence

Sacred Heart arts and science college, perani, India.

Corresponding Author Email: florencereni9494@gmail.com

Abstract. The biological properties of nanomaterials depend on their crystalline nature, size, and shape. In this present work, spherical-shaped zirconia nanoparticles (ZrO₂ NPs) with an average size of 10-15 nm were fabricated and their antibacterial and anticancer activities evaluated. *Enicostemma littorale* (*E. littorale*) whole plant extract was used as a reducing agent for the green synthesis of ZrO₂-NPs. UV-Visible spectrophotometer (UV-Vis), X-ray diffraction pattern (XRD), Fourier transform infrared spectrophotometer (FTIR), transmission electron microscopes (TEM) coupled with selected area diffraction (SAED), and scanning electron microscope coupled with energy dispersive study (EDS) were used to characterise the synthesized ZrO₂ NPs. Results established the proficient anticancer activity of the synthesized ZrO₂ NPs towards cell lines as well as efficient antibacterial activity. This is the first study in which a whole plant extract of *E. littorale* was used to synthesize spherical ZrO₂ NPs for enhanced antibacterial and anticancer activities. Good electrochemical performance and the flow of ions were observed from the electrochemical study.

Keywords: *Enicostemma littorale*, ZrO₂, Anticancer activity, Green synthesis, Morphology.

1. INTRODUCTION

Due to its simple and eco-friendly methodology, green synthesis has been adopted recently as a substitute to the chemical methods used to synthesize metal oxide nanoparticles. Green approaches to nanomaterial synthesis are significant because of their environmental friendliness, low cost, physical and chemical properties, and industrial applications [1, 2]. Metal zirconium oxide is a good material which has been extensively used in the reinforcement of structures, antibacterial agents, and dye degradation [3]. Zirconia is widely used in electrochemical capacitors, micro-electronics, anti-corrosive coatings, used in sensors, catalysis, fuel cells, and magnetic materials [4, 5]. Various chemical methods such as precipitation, solvothermal, sonochemical, hydrothermal, and sol-gel methods [6, 7] are some of the chemical methods engaged in the synthesis of nanoparticles. However, the conventional methods require toxic chemicals, which produce harmful effects on human beings and the environment [8]. Zirconia is an n-type semiconductor and can be used as an insulator due to its crystalline structure [9]. Applications of zirconia depend on their crystal's shape and size. Hence, spherical-shaped zirconias have been tested for oxygen sensors, fuel cell electrolytes, and gate dielectrics [10]. Various natural sources have been used as reducing agents in green synthesis. Plant extracts, bacteria, and fungi are used in the green synthesis of zirconia NPs [11]. Ahmed et al. synthesized zirconia NPs using *Enterobacter sp.* and evaluated their antifungal activity [12]. *Fusarium Oxysporum* stabilized zirconia NPs have been reported [13]. Various plants, such as *Anacardium occidentale* leaf extract [14], *Aloe vera* gel [15], *Curcuma longa* tuber extract [16], *Nephelium lappaceum L* fruit extract [17], and *Euclea natalensis* extract [3], have been used as natural reducing agents for the evaluation of antibacterial, antifungal, antioxidant, and photocatalytic activities. However, the whole plant extract of *Enicostemma littorale* has not been used for the green synthesis of zirconia nanoparticles. *Enicostemma littorale* is a well-known anti-diabetic drug [18]. The plant contains various phytochemicals such as glycosides, phytosterol, glucosides, sugars, and tannins [19, 20]. This plant extract has been used to cure jaundice and is also used as an anti-pyretic drug [21]. Antibacterial activity of this whole plant's extract has been proven for its bactericidal activity against many pathogenic bacteria [22]. Although many plant extracts have been used as natural reducing agents, *E. littorale* has

not been used for the green synthesis of zirconia NPs. In the present work, green synthesized zirconia nanoparticles using whole plant extract of *E. littorale* at various concentrations were carried out. Anticancer activity was tested by the MTT (3-(4, 5-dimethylthiazol-2-yl)-2, 5-diphenyltetrazolium bromide) assay against human cancer cell lines. In addition to that, the electrochemical performance of the samples was also studied.

2. MATERIALS AND METHODS

Materials: *Enicostemma littorale* was collected near Tiruvannamalai, Tamil Nadu. Zirconium oxychloride ($ZrOCl_2 \cdot 8H_2O$), MTT (3-(4, 5-dimethylthiazol-2-yl)-2, 5-diphenyltetrazolium bromide), and other chemicals were purchased from LoboChemie Ltd., Mumbai, India. All the chemicals were used without further purification. Distilled water was used to prepare the salt solutions. Human skin cancer cell lines (A 431) and bacterial cultures were obtained from Coimbatore Medical College Hospital, Coimbatore, Tamil Nadu. An electrochemical study was carried out at St Joseph College, Trichy, Tamil Nadu, India.

Extract preparation: Freshly collected *E. littorale* was washed thoroughly with running tap water followed by distilled water, then cut into small pieces and dried in the shade. The dried leaves were powdered using an electric mixer. 50 g of powder was put in 200 mL of distilled water and boiled for 1 hour at 100°C. A dark brownish extract was obtained. The extract was filtered and concentrated at 80°C for 1 h on a hot plate and stored in the refrigerator for further use.

Synthesis of ZrO_2 NPs: Three different concentrations of zirconium oxychloride solution were prepared in 100 ml of distilled water. Zirconyl oxychloride solutions (0.02, 0.04, and 0.06M) and the extract (30, 50, and 70 mL) were pre-heated at 80°C. Zirconyl oxychloride solution (was placed on a magnetic stirrer. The extract (30 mL) in hot condition was dropwise added to the zirconyl oxychloride solution. The formed precipitate was thoroughly washed with distilled water and centrifuged at 5000 rpm for 20 min. Then, the precipitate was washed with ethanol and acetone to remove any organic impurities and dried at 80°C in a hot air oven. The lumps were crushed into powder and annealed at 500°C for 3 h in a muffle furnace to get crystalline zirconia NPs. The ZrO_2 NPs synthesized 0.02, 0.04 and 0.06 M zirconyl oxychloride solutions were named Zr0.02, Zr0.04 and Zr0.06.

Anticancer activity: The skin cancer cell line (A 431) was obtained from the National Centre for Cell Science (NCCS), Pune and grown in Eagles Minimum Essential Medium containing 10% foetal bovine serum (FBS). The cells were maintained at 37°C with 5% carbon dioxide. The monolayer cells were detached with trypsin-ethylene diaminetetraacetic acid (EDTA) to make single cell suspensions, and viable cells were counted using a hemocytometer and diluted with medium containing 5% FBS to give a final density of 1×10^5 cells/ml. 96-well plates were seeded with 1×10^4 cells per well and incubated at 37°C with 100% relative humidity. They were dissolved in dimethylsulfoxide (DMSO) and an aliquot of the sample solution was diluted to twice the desired final maximum test concentration with serum free medium. Aliquots of 100 μ L of Zr0.02, Zr0.04, and Zr0.06 were added to the wells containing 100 μ L of medium. The plates were incubated for an additional 48 h at 37°C. The medium without a sample was considered a control and triplicate was maintained for all concentrations. 3[4,5-dimethylthiazol-2-yl] 2,5-diphenyltetrazolium bromide (MTT), 15 μ L of MTT (5 mg/mL) in phosphate buffered saline (PBS) was added to each well and incubated at 37°C for 4 h. The medium with MTT was then flicked off and the formed formazan crystals were solubilized in 100 μ L of DMSO and then the absorbance was measured after 48 h of incubation at 570 nm using a microplate reader [23, 24].

Characterization methods: Powder X-ray diffractometer (XRD, SMART Bruker D8 Advance X-ray diffractometer) irradiated with Cu K radiation ($\lambda = 1.540 \text{ \AA}$) and the 2θ angle from 20-80° was used to characterise the crystalline phase of zirconia NPs. The XRD pattern was matched with JCPDS data using previous reports and software. Surface morphology and elemental composition analysis were carried out by a scanning electron microscope fitted with a coupled energy dispersive study (TESCAN OXFORD, VEGA 3 INCA software) using an acceleration voltage of 30 KeV. The size and shape of nanoparticles were assessed by using a transmission electron microscope coupled with a selected area electron diffraction (SAED) pattern was recorded by using a transmission electron microscope (TEM, TECNAI G2 S-Twin operated at an accelerating voltage of 200 KeV). The functional groups and the metal-oxygen bond were identified by using a Fourier Transform Infrared spectrometer (PerkinElmer spectrum 100 FTIR) in the wavenumber range from 4000-400 cm^{-1} . A UV-Visible spectrum was recorded (JASCO-V-670, Shimadzu) spectrophotometer in the wavelength range of 200-800 nm.

Electrochemical study: An electrochemical study was carried out according to the procedure cited in the literature. Three electrodes were used to obtain the results. Pt wire was used as a counter electrode and Ag/AgCl was used

as a working electrode. For this experiment, ZrO₂ NPs were coated on glassy carbon using 0.5 mL of ionic conductivity solution with ethanol and ultra-sonicated with ZrO₂ NPs for 30 min, and solutions were pipetted onto the electrode and dried. Electrolytes like KCl and NaNO₃ (2 M) were used to measure the Cyclic voltammeter (CV) at the scan rates of 100, 50, 30, 20 and 10 mV/s. The electrochemical impedance spectrum was recorded at a frequency range of 100 kHz to 0.01 Hz [4].

3. RESULTS AND DISCUSSION

Green synthesis of zirconia NPs: The whole plant extract of *Enicostemma littorale* was effectively used as a green reducing agent. The concentration of extract was optimized according to the concentration of zirconyl oxychloride and was 30, 50, and 70 mL. Pre-heated salt solution and extract were mixed thoroughly on a magnetic stirrer. The UV spectrum of green synthesized ZrO₂ NPs is shown in Figure 1. The maximum absorption (λ_{\max}) peak was 297, 299, and 302 nm for 0.02, 0.04, and 0.06 M zircon oxychloride solutions. The estimated bandgap energy of Zr0.02, Zr0.04, and Zr0.06 were found to be 3.34, 3.31, and 3.40 eV, respectively [25].

Functional group analysis: An FTIR spectrum was recorded to analyze the functional groups of ZrO₂ NPs (Figure 2). The results revealed that the broad band around 3429 cm⁻¹ is attributed to the OH group on the surface of the nanoparticles [26]. A small absorption band at 611 cm⁻¹ is attributed to Zr–O–Zr stretching vibration, which indicates the presence of the tetragonal phase [27]. The peak at 1021 cm⁻¹ revealed Zr–O binding bands that were characteristic of the tetragonal structure [28, 29]. The O–H stretching and bending vibrations are observed at 1655 and 1466 cm⁻¹ [17] are attributed to the presence of moisture content. The FTIR spectrum confirms that no characteristic peak is responsible for the organic molecules, which suggests that the organic molecules decomposed during the annealing at 500°C. Although the water-soluble organic molecules acted as reducing agents, organic molecules were removed from the surfaces after annealing at 500°C.

XRD pattern analysis: Figure 3 shows the XRD pattern of ZrO₂ NPs. As shown in Figure 3, the diffraction peaks at 30.66, 35.16, 50.43, and 60.36° correspond to tetragonal phases of ZrO₂ NPs to PDF 49-1642 [30]. The XRD peaks can be indexed for the planes of (101), (002), (200), and (211). However, no peak was observed for the monoclinic phase. The results revealed that the ZrO₂ NPs was in the tetragonal phase. The diffraction peaks that appear for ZrO₂ NPs synthesized from 0.02, 0.04, and 0.06 M precursor solutions are broad due to their amorphous nature. Scherrer's formula was utilized to compute the crystallite sizes from the full width of the half-maximum (FWHM) peak broadening of the (111) peak of the XRD patterns.

$$D = \frac{0.9\lambda}{\beta \cos\theta} \dots\dots\dots(1)$$

is the X-ray wavelength (0.1542 nm), the angular line width of full width half-maximum (FWHM) intensity, and Bragg's angle. The crystallite size was determined from the most intense peak in the (101) plane. There is no significant difference in the XRD pattern of ZrO₂ NPs synthesized using different concentrations of extract. The strength of zirconyl oxychloride increasing with increasing concentration of extract may be the reason for this similarity in the XRD pattern. The average crystallite size of Zr0.02, Zr0.04, and Zr0.06 was found to be 42, 37, and 41 nm, respectively.

SEM image analysis: The morphology of the ZrO₂ NPs synthesized via the green route was analyzed through SEM analysis to confirm the consistence of the crystalline phase by XRD analysis. In SEM images of all the samples, uneven distributions of particles are observed with agglomeration, which are spherical in shape (Figure 4). The majority of nanocrystal growth occurs through aggregation during calcinations. However, biomolecules present in the extract are involved in the formation of nanoparticles. The formation of nanoparticles also depends on the nature of biomolecules as well as the concentration of the extract [31]. The EDAX spectrum shows peaks corresponding to zirconium and oxygen, thus exhibiting the purity of nanoparticles.

TEM morphology study: The morphology, shape, and size of the green synthesized nanoparticles were analyzed by TEM images. As shown in Figure 5, spherical-shaped particles were found to be uniformly distributed in three samples. According to the TEM images, the average crystallite size of the Zr0.02, Zr0.04, and Zr0.06 was found

to be 8.14, 9.10, and 8.09 nm, respectively. Figure 5 (iv) shows the selected area diffraction pattern. The lattice fringes obtained from the SAED pattern confirm that the particles are of crystalline nature.

Anticancer activity: As part of the application, ZrO₂ NPs were tested for their anticancer activity against human carcinoma cancer cell lines (A431). The results of the research revealed that nanoparticles were effective in inhibiting the growth of cancer cells. However, the anticancer activity was in a dose-dependent manner, as displayed in Figure 6. The concentration of Zr0.02, 0.04, and Zr0.06 were tested at 6.5, 12.50, 25.0, 50.0, and 100 µg/mL. The IC₅₀ values of Zr0.02, Zr0.04 and Zr0.06 were 44.25, 36.49 and 39.62 µg/mL, respectively. The results show that the cell viability was increased with an increasing the concentration of nanoparticles. The microscopic images revealed that nanoparticles disrupt the cell membrane and kill A431 cancer cells (Figure 7), whereas untreated cells (control cells) tend to appear intact, as displayed in Figure 7 (Zrc). The cell viability (Figure 6) and IC₅₀ curves for A431 reveal that nanoparticles synthesized using *E. littorale* extract are found to be more toxic to the cell lines. It can be understood that nanoparticles are toxic to cell lines and have potential in the development of anticancer drugs. The result shows that cell mortality is induced by loss of membrane integrity of the cell lines. The IC₅₀ curves confirmed the results of the MTT assay [32].

Formation mechanism of zirconia nanoparticles: The formation of ZrO₂ NPs proceeds through three different steps: reduction of metal ions, aggregation of nanoparticles, and the subsequent growth of nanoparticles. However, each step depends on the nature of the reducing agent, concentration, and the reaction conditions. A feasible mechanism also depends on the nature of the biomolecules present in the whole plant extract of *E. littorale* [22]. Many important compounds such as iridoid glycosides, flavonoids, and xanthone may be responsible (OH group) for the reduction metal ions. This plant was found to contain The OH groups present in the biomolecules of the *E. littorale*'s extract react with zirconyl oxychloride. The zirconium hydroxide is formed first. After annealing at a particular temperature (500°C), hydroxide is converted into ZrO₂ NPs. During the calcinations, organic molecules and other impurities are removed [33].

Electrochemical study: The electrochemical results were observed under electrochemical impedance spectroscopy and the cyclic voltogram (CV) of ZrO₂ NPs electrolytes is displayed in Figure 8. The CV of ZrO₂ NPs modified with an electrical conductivity solution result in a rectangular shape, which exhibits capacitive behaviour [34]. Figure 8 show that the increase in the scan rate increases the current flow due to the resistance effects [35]. When the scan rate increases, it decreases the capacitance of Zr0.02, Zr0.04 and Zr0.06 due to porosities and higher specific surface area. However, the increase in ionic resistivity of ZrO₂ NPs decreases the capacitance of the electrode at the higher scan rate of 100 mVs⁻¹. This may be due to the slower transfer rate of ions, which causes the saturation of protons during the redox process. Hence, ZrO₂ NPs can be suitable candidate for fuel cell application [36].

4. CONCLUSION

This work reports the green syntheses of [36]. Biomolecules present in the aqueous extract of *E. littorale* were used to convert zirconyl oxychloride into zirconium hydroxide. The synthesized [36]. were tetragonal crystalline structures (XRD). According to the TEM, the average particle size was 9 nm. These nanoparticles were used as anticancer agents. It was noticed that green synthesized nanoparticles are biocompatible nanostructures with anticancer activity against skin cancer cells (A431). Further investigation is required to discover the molecular mechanisms of these nanoparticles against cancer cell lines. Green synthesis of ZrO₂ NPs is an eco-friendly method that could be used for the development of nanomaterials for biomedical applications.

Declaration of Competing Interest: The authors declare that there are no conflicting interests.

Acknowledgement: The author (P.S) gratefully acknowledges Dr. R. Subramanian, ex-Professor of Sun Arts and Science College, Tiruvannamalai, for proof reading and corrections. The same author thanks National College, Trichy, for providing characterization facilities.

REFERENCE

1. Beydoun, Donia, Rose Amal, Gary Low, and S. McEvoy. "Role of nanoparticles in photocatalysis." *Journal of Nanoparticle Research* 1 (1999): 439-458.
2. Bundschuh, Mirco, Juliane Filser, Simon Lüderwald, Moira S. McKee, George Metreveli, Gabriele E. Schaumann, Ralf Schulz, and Stephan Wagner. "Nanoparticles in the environment: where do we come from, where do we go to?" *Environmental Sciences Europe* 30, no. 1 (2018): 1-17.

3. Petros, Robby A., and Joseph M. DeSimone. "Strategies in the design of nanoparticles for therapeutic applications." *Nature reviews Drug discovery* 9, no. 8 (2010): 615-627.
4. Husen, Azamal, and Khwaja Salahuddin Siddiqi. "Phytosynthesis of nanoparticles: concept, controversy and application." *Nanoscale research letters* 9 (2014): 1-24.